

*Curcumin/Tween 20-incorporated
cellulose nanoparticles with enhanced
curcumin solubility for nano-drug delivery:
characterization and in vitro evaluation*

Article

Accepted Version

Ching, Y. C., Gunathilake, T. M. S. U., Chuah, C. H., Ching, K. Y. ORCID: <https://orcid.org/0000-0002-1528-9332>, Singh, R. and Liou, N.-S. (2019) Curcumin/Tween 20-incorporated cellulose nanoparticles with enhanced curcumin solubility for nano-drug delivery: characterization and in vitro evaluation. *Cellulose*, 26 (9). pp. 5467-5481. ISSN 5467–5481 doi: 10.1007/s10570-019-02445-6 Available at <https://centaur.reading.ac.uk/102062/>

It is advisable to refer to the publisher's version if you intend to cite from the work. See [Guidance on citing](#).

To link to this article DOI: <http://dx.doi.org/10.1007/s10570-019-02445-6>

Publisher: Springer

All outputs in CentAUR are protected by Intellectual Property Rights law, including copyright law. Copyright and IPR is retained by the creators or other copyright holders. Terms and conditions for use of this material are defined in

the [End User Agreement](#).

www.reading.ac.uk/centaur

CentAUR

Central Archive at the University of Reading

Reading's research outputs online

[Click here to view linked References](#)

Curcumin/Tween 20-incorporated cellulose nanoparticles with enhanced curcumin

solubility for nano-drug delivery: characterization and in vitro evaluation

Yern Chee Ching· Thennakoon M. S. U. G.· Cheng Hock Chuah· Kuan Yong Ching· Ramesh Singh· Nai-Shang Liou

a Department of Chemical Engineering, Faculty of Engineering, University of Malaya, 50603 Kuala Lumpur, Malaysia

b Department of Chemistry, Faculty of Science, University of Malaya, 50603 Kuala Lumpur, Malaysia

c University of Reading Malaysia, Persiaran Graduan, Kota Ilmu, Educity, 79200 Iskandar Puteri, Johor, Malaysia

d Department of Mechanical Engineering, Faculty of Engineering, University of Malaya, 50603 Kuala Lumpur, Malaysia

e Department of Mechanical Engineering, Southern Taiwan University of Science and Technology, 710 Tainan City, Taiwan, ROC

Abstract

A poorly water-soluble anticancer drug, curcumin was loaded in to cellulose nanocrystals by dissolving it in a commonly used nonionic surfactant medium. Results showed that the drug loading capacity of nanocellulose increased with increasing the surfactant concentration of the medium. The drug loading capacity of nanocellulose in surfactant medium was significantly higher (7.73mg/g) when compared to the drug loading capacity (3.35mg/g) in methanolic medium. The nanocellulose drug loaded in surfactant medium (TW/CNC) showed higher drug release compared to the nanocellulose drug loaded in methanolic medium (METH/CNC). It was 8.99 mg/L for TW/CNC and 2.65 mg/L for METH/CNC in simulated gastric fluid. Due to the increased stability of curcumin in acidic medium, all the nanoparticles showed higher drug release in simulated gastric fluid compared to phosphate buffered saline solution. The maximum dissolution of curcumin was 2.13 mg/mL in distilled water containing 4% (w/v) of surfactant. UV-visible spectra revealed that the curcumin retained its chemical activity after in vitro release. From these findings, it is believed that the incorporation of curcumin into nanocellulose in surfactant medium provides a promising approach for delivery of curcumin to stomach and upper intestinal tract.

Key words: Nanocellulose, Curcumin, Tween 20, Bioavailability

Introduction

Nanotechnology is playing a key role in a broad range of applications. Since its introduction, it is a key component of advancing almost all areas of science, particularly, drug delivery and formulation. Today, nanotechnology is being applied in the areas of drug delivery and formulations known as 'Nanopharmaceutics'. As nanoparticles are accepted by cells more effectively than larger microparticles, they can be used as efficient transport and delivery systems. Nanostructured-based drug delivery systems offer many advantages over conventional drug delivery systems, including their ability to pass through the narrow capillary vessels due to their smaller size, ability to penetrate cells and tissue gap to arrive at target organs and to provide controlled drug release over a prolong period (Rizvi and Saleh 2017). Nanoparticles exhibit greater drug uptake compared to microparticles. The small dimensions of nanoparticles compared to their bulk counterparts bring drug more closer to the surface of the particle, which results in faster drug release (Rizvi and Saleh 2017). With the increase in potential usefulness of nanoparticles in therapeutics delivery, knowledge on the health effects of the nanoparticle exposure and the basics of the interaction of nanoparticles with living cells, organs and organisms is still limited. In this respect, materials and strategies which minimize the possibilities of causing adverse and toxic effects have been developed for therapeutic delivery, in particular the choice of biodegradable nanoparticles with a limited life span which avoid the accumulation in the liver and spleen (Gustafson et al. 2015).

Nanocellulose is a biodegradable nanomaterial which is obtained by most abundant natural polymer on earth. Nanocelluloses and their derivatives are attractive candidates for controlled drug delivery systems due to their biocompatibility, biodegradability and stimuli-responsiveness. It has been investigated for the delivery of protein, poorly water soluble drugs such as

72 beclomethasone, dipropionate, indomethacin and itraconazol from previous studies (Löbmann
73 and Svagan 2017). The unique physico-chemical, rheological and barrier properties of
74 nanocellulose provide them to stabilize air/water and oil/water interfaces (Löbmann and Svagan
75 2017). Also, their large surface area-to-volume ratios offer possibilities for positive molecular
76 interactions with poorly-soluble drugs. The acid hydrolysis is an economical method that have
77 been extensively used for nanocellulose extraction from various natural sources such as plant
78 fiber, wood fiber, microcrystalline cellulose, algae, tunicate and bacteria. Nanocellulose
79 synthesized using acid hydrolysis has a size range from 10 nm to 350 nm (Phanthong et al. 2015;
80 Sadeghifar et al. 2011; Sampath et al. 2017). Numerous studies have reported relationship
81 between nanoparticle size and biological adverse effects (Gustafson et al. 2015). From the
82 literature it was reported that the optimum size for nanoparticle as carriers for drug delivery is
83 approximately 100 nm (Rizvi and Saleh 2017). Thereby, acid hydrolysis can be used to produce
84 the nanocelluloses with optimal size which is suitable for drug delivery.

85 Curcumin is a polyphenol obtained from the plant *Curcuma longa*. Curcumin has received
86 worldwide attention due to its promising anti-cancer properties (Ibrahim et al. 2018). Also, it can
87 cause a high rate of *Helicobacter pylori* eradication which was identified as a group I
88 carcinogenic agent of human gastric cancer (De et al. 2009; Santos et al. 2018). However, the
89 complete potential of curcumin has not been successfully utilized due of its poor water solubility
90 and low bioavailability. Several strategies have been developed to enhance the solubility and
91 bioavailability of curcumin such as formation of micelles, nanosuspensions, nanoparticles and
92 nano-emulsions are some of them (Kamaraj et al. 2018). Solid dispersion is one of efficient
93 method to overcome the challenges associated with poor water solubility of drugs. However the
94 miscibility and stability of the dispersion are main limitations related with the development of

95 solid dispersions. The use of surfactant in solid dispersion can overcome these limitations
96 (Chaudhari and Dugar 2017). Surfactants can be cationic, anionic, nonionic or amphoteric. When
97 surfactant molecules are dissolved in water at a concentration greater than critical micelle
98 concentration (cmc), they form spherical form of aggregates known as micelles. The solubility of
99 hydrophobic drugs in nonionic surfactant solutions is greater than compared to solubility in ionic
100 surfactant solutions, because of their lower cmc values (Rangel-Yagui et al. 2005). In a micelle,
101 the hydrophobic tails of several surfactant molecules flock into oil-like core in order to minimize
102 their contact with water, and the hydrophilic heads region faces the outside surface of the micelle
103 in order to maximize their contact with water.

104 Although research on nanocellulose based drug delivery systems are exponentially growing,
105 there are a few reports that have been published on nanocellulose/curcumin drug delivery
106 systems (de Castro et al. 2018; Mohan Yallapu et al. 2012; Ntoutoume et al. 2016). Inspired by
107 our previous work (Gunathilake et al. 2018; Udeni Gunathilake et al. 2017), we continued our
108 investigation on the enhancement of bioavailability of curcumin. From our previous study,
109 curcumin and nonionic surfactant were incorporated into nanocellulose reinforced chitosan
110 hydrogel and studied the drug delivery behavior. We observed that the cumulative drug release
111 of the hydrogel increased with increasing the nonionic surfactant concentration. However, the
112 drug loading efficiency of the hydrogel decreased with the incorporation of the surfactant to the
113 hydrogel (Gunathilake et al. 2018). Furthermore, the addition of nanocellulose enhanced the
114 mechanical strength and swelling behavior of the hydrogel (Sampath et al. 2017). However, the
115 problems encountered in previous study were the decrease of encapsulation efficiency of the
116 drug with increasing of surfactant concentration and incomplete drug release profiles. Polymer
117 phase of chitosan hydrogel acted as a diffusion barrier against movement of drug in the previous

study. Due to the hydrophilic property of the surfactant (high HLB value), the intake of water has narrowed the diffusion barrier. Hence the entrapment efficiency decreased with increasing of surfactant. In this study, the increase of surfactant concentration will improve the micelle formation and it will facilitate incorporation of drug into nanocellulose and hence, result in improvement of encapsulation efficiency. Previous study showed incomplete drug release profiles over the time of monitoring. This is due to the fact that the embedded drug released slowly over a longer period of time by diffusion through the hydrogel matrix. In this study, the small dimensions of nanoparticles bring drug closer to the surface of the nanocellulose particles which results in faster drug release. This will lead to complete drug release during shorter residence time of the dosage form in the stomach. Therefore, the curcumin/Tween 20 incorporated cellulose nanoparticle system will provide a better platform to overcome the problems associated with the curcumin/nanocellulose reinforced chitosan hydrogel system as described in our previous study (Gunathilake et al. 2018).

In this study, we dissolved hydrophobic drug (curcumin) in a commonly used nonionic surfactant solution and incorporated in to nanocellulose, which synthesized from microcrystalline cellulose by sulphuric acid hydrolysis method. Depending on the arrangement of hydrophobic and hydrophilic groups of surfactant molecules in the micelle structure, there may be different interactions can occur with drug molecules and cellulose nanocrystals. Hydrophobic drug (curcumin) may be located in the inner core of the micelle of nonionic surfactant and the hydrophilic groups of nonionic surfactants may have affinity for adsorption to cellulose, because of its hydroxyl groups. Tween is a non-ionic surfactant commonly used in drug delivery applications for dispersing of hydrophobic drugs. They consist of two different groups: a hydrophilic head group and a hydrophobic alkyl chain. Based on the alkyl chain length, there are

different types of Tween surfactants namely, Tween 20, 40, 60 and 80. The differences of the alkyl chain length of surfactants influence the hydrophile–lipophile balance (HLB) value of the surfactant and the entrapment efficiency of drug delivery systems. Increasing the alkyl chain length (the surfactants with lower HLB values) is leading to higher entrapment efficiency. The higher the chain length (surfactants with lower HLB values), would cause lower release rates of hydrophobic drugs. This is due to the fact that the surfactants having lower HLB values are more lipophilic and less water soluble. But, the surfactants with higher HLB values such as Tween 20 (HLB= 16.7) helps to improve the release rates of hydrophobic drugs to a desired extent. According to the findings of this study, we envision that our proposed curcumin/nonionic surfactant-incorporated cellulose nanoparticle drug delivery system has great potential for enhancing the bioavailability of curcumin.

Experimental methodology

Materials

Microcrystalline cellulose, Tween 20 and phosphate-buffered saline were supplied by R&M chemicals (Essex, UK). Sodium chloride, hydrochloric acid, methanol and sulfuric acid were purchased from Friendemann Schmidt Chemicals (Parkwood, Australia). The drug curcumin was provided by HIMEDIA laboratories Pvt Ltd. (Mumbai, India).

Methodology

Extraction of curcumin from turmeric

Curcumin was extracted from turmeric (rhizomes of *Curcuma longa*) by solvent extraction method. Rhizomes were dried, crushed and soaked in methanol for 3 days. After that, the extract

was filtered with Whatman filter paper (pore size 0.2 μm). Finally, the filtrate was evaporated under vacuum to obtain semi-dry oily mass.

FTIR study

The FTIR spectra of curcumin extracted from rhizomes of curcuma longa, Tween 20, nanocellulose and curcumin loaded nanocellulose were obtained using PerkinElmer spectrum 400 FTIR spectrometer over the range 4000–400 cm^{-1} .

X-ray diffraction

The crystallinity degrees of curcumin, nanocellulose and curcumin incorporated nanocelulosewere studied using X-ray diffractometer (PANalytical EMPYREAN diffractometer). The samples were dried and powdered before they were analyzed. The samples were exposed to Cu K α radiation generated at 40 mA, 40 kV, a 2 θ angle of 5-60°, and a scan rate of 6°/min.

Drug loading

Cellulose nanocrystals (CNC) were synthesized by sulfuric acid hydrolysis of microcrystalline cellulose, as reported in our previous study (Sampath et al. 2017). To prepare curcumin loaded nanocellulose in Tween 20 medium, excess amount of curcumin were mixed with different concentrations of Tween 20 (0.8%, 1.6%, 2.4%, 3.2%, 4%, 4.8%, 5.6% (w/v)) and stirred for 24 h. Then, the curcumin solutions (in Tween 20 medium) were centrifuged (10,000 rpm for 10 min) and supernatants were collected. After that, a constant amount of nanocellulose was mixed with each curcumin solution (in Tween 20 medium) and stirred for 24 h. To prepare curcumin loaded nanocellulose in methanolic medium, constant amount of nanocellulose (similar to use in

Tween medium) was mixed with different concentrations (similar to the dissolved amount of curcumin present in Tween 20 solutions) of curcumin solutions (prepared by dissolving curcumin in methanol and diluting with distilled water) and stirred 24 h. After that, the suspension was centrifuged 6000 rpm for 20 min and supernatant was decanted and the remaining amount of curcumin was determined using UV-Vis spectroscopic method. The drug loading capacity was calculated based on the ratio of the absorbed amount of the drug from the solution to the weight of the nanocellulose (Eq. (1)).

$$\text{Drug loading capacity} = \frac{\text{Absorbed amount of drug from the solution}}{\text{Weight of nanocellulose}} \quad (1)$$

Drug release

In vitro drug release from drug loaded nanocellulose was studied in simulated gastric fluid (SGF) (prepared by dissolving 2 g NaCl in 7.0 mL HCl and water up to 1000 mL) and phosphate buffer saline solution (PBS) at 37 °C. In order to study the release, at prefixed time intervals, 3 mL of medium was withdrawn and returned it back to the solution after the analysis. The concentration of curcumin was determined using UV-Vis spectroscopic method. The experiments were replicated three times and average values were taken. The types of nanocellulose used for drug release studies are as per the details mentioned in Table 1.

Table 1 Types of nanocellulose used for the drug release studies (based on the drug loading and releasing medium).

Types of nanocellulose (based on the drug loading and releasing medium)	Weight of nanocellulose (g)	Amount of drug (curcumin) loaded per 1 g of nanocellulose (mg)	Drug loading medium	Drug releasing medium
TW/CNC-SGF	1	7.73	Aqueous solution of Tween 20	Simulated gastric fluid

TW/CNC-PBS	1	7.73	Aqueous solution of Tween 20	Phosphate buffered saline solution
METH/CNC-SGF	1	3.35	Methanolic medium	Simulated gastric fluid
METH/CNC-PBS	1	3.35	Methanolic medium	Phosphate buffered saline solution

Solubility studies of curcumin in distilled water

To determine the solubility of curcumin in distilled water, an excess amount of curcumin extract was added to 30 mL of distilled water and mixed with different concentrations of Tween 20 (0.8%, 1.6%, 2.4%, 3.2%, 4%, 4.8%, 5.6% (w/v)). Then, the mixtures were stirred (350 rpm) using magnetic stirrer for 12h. Samples were covered in order to prevent photo-degradation. After that, the solutions were centrifuged (10,000 rpm for 10 min) to separate the undissolved curcumin and the dissolved curcumin was determined using UV-Vis spectroscopic method.

Drug activity

The drugs are often inevitable and therefore, the chemical reactivity related to biological activity of the drug is most important parameter to be concerned when selecting a drug delivery carrier. The UV-Vis spectra of pure drug and released drug can be used to determine if any deterioration reaction happened due to the destructive interactions between drug and carrier molecules (Bashir et al. 2016). The UV-visible spectra of pure drug and the drug released from the cellulose nanoparticles were obtained by scanning the drug solutions using UV-visible spectrophotometer (scan range 300-800 nm). Drug activity was determined by comparing the spectra (the absorption maxima (λ_{max})) of pure drug and drug released from nanocellulose.

Results and discussion

FTIR study

Fig. 1 displays the FTIR spectra of curcumin, nonionic surfactant, nanocellulose, drug loaded nanocellulose in surfactant medium and drug loaded nanocellulose in methanolic medium. The IR spectrum of curcumin derived from turmeric is more similar to the IR spectrum of crystalline curcumin derived from turmeric powder, which was reported in previous studies (Bich et al. 2009; Fugita et al. 2012). From our previous study, we have compared and characterized the FTIR spectra of extracted curcumin and curcumin purchased from Himedia Co. (Gunathilake et al. 2018). In the FTIR spectrum of curcumin, the highest frequency bands observed within 2700-3000 cm^{-1} region are assigned to the aromatic C-H stretches (Kolev et al. 2005). The IR bands at 815 cm^{-1} and 720 cm^{-1} belongs to the $\nu(\text{C-H})$ out of plane vibration of the aromatic ring (Kolev et al. 2005). In the range of 700-500 cm^{-1} , we could see deformation vibrations of both benzene rings and the out of plane vibrations of both OH groups, which are at 607 cm^{-1} and 546 cm^{-1} (Bich et al. 2009). These aromatic groups provide much of the hydrophobicity to the curcumin molecules. Due to these hydrophobic groups, curcumin molecules are located in the core of the surfactant micelles, when it dispersed in surfactant solution. The peak at 1679 cm^{-1} appeared due to the C=O vibrations (Bich et al. 2009). The most prominent band in the IR spectrum is at 1509 cm^{-1} can be attributed to highly mixed vibrations ($\nu\text{C=O}$, $\delta\text{CC}^{10}\text{C}$, $\delta\text{CC=O}$) (Bich et al. 2009). These ketone group exhibits keto-enol tautomerism forming a predominant keto form in acidic and neutral media and stable enol form in alkaline medium. Therefore, it is insoluble in water under acidic or neutral pHs but dissolves in alkaline conditions (Jankun et al. 2016).

241 In the FTIR spectrum of the **nonionic surfactant**, the peak around 3522 cm^{-1} is due to the
 242 hydrogen bonded O-H stretching vibrations. The peaks at 2935 cm^{-1} and 2883 cm^{-1} are due to the
 243 asymmetric and symmetric methylene stretching vibrations. The 1741 cm^{-1} peak represents the
 244 carbonyl group from R-CO-O-R and the peak at 1667 cm^{-1} attributed to the carbonyl stretching.
 245 The most prominent peak at 1103 cm^{-1} is due to the stretching vibration of $-\text{CH}_2-\text{O}-\text{CH}_2-$ (Ortiz-
 246 Tafoya and Tecante 2018).

247 In the FTIR spectrum of nanocellulose, the broad band at 3334 cm^{-1} is due to the characteristic –
 248 OH stretching from vibrations in the intra-and intermolecular hydrogen-bonded hydroxyl groups
 249 (Gunathilake et al. 2017). The band at 2901 cm^{-1} is corresponded to aliphatic saturated CH-
 250 stretching in the glucose units. Other peaks detected include the adsorption band at 1636 cm^{-1}
 251 which is due to the absorption of water onto cellulose, the peak at 1428 cm^{-1} associated with
 252 CH_2 symmetrical bending and scissoring motion in cellulose, the peak at 1159 cm^{-1} is due to the
 253 asymmetrical bridge C–O–C stretching from the glycosidic bond, the band at 1029 cm^{-1}
 254 representing stretching of the glucopyranose unit and the peak at 896 cm^{-1} is typical of the β -
 255 glycosidic linkage in cellulose (Ching & Ng 2014, Sahlin et al. 2018).

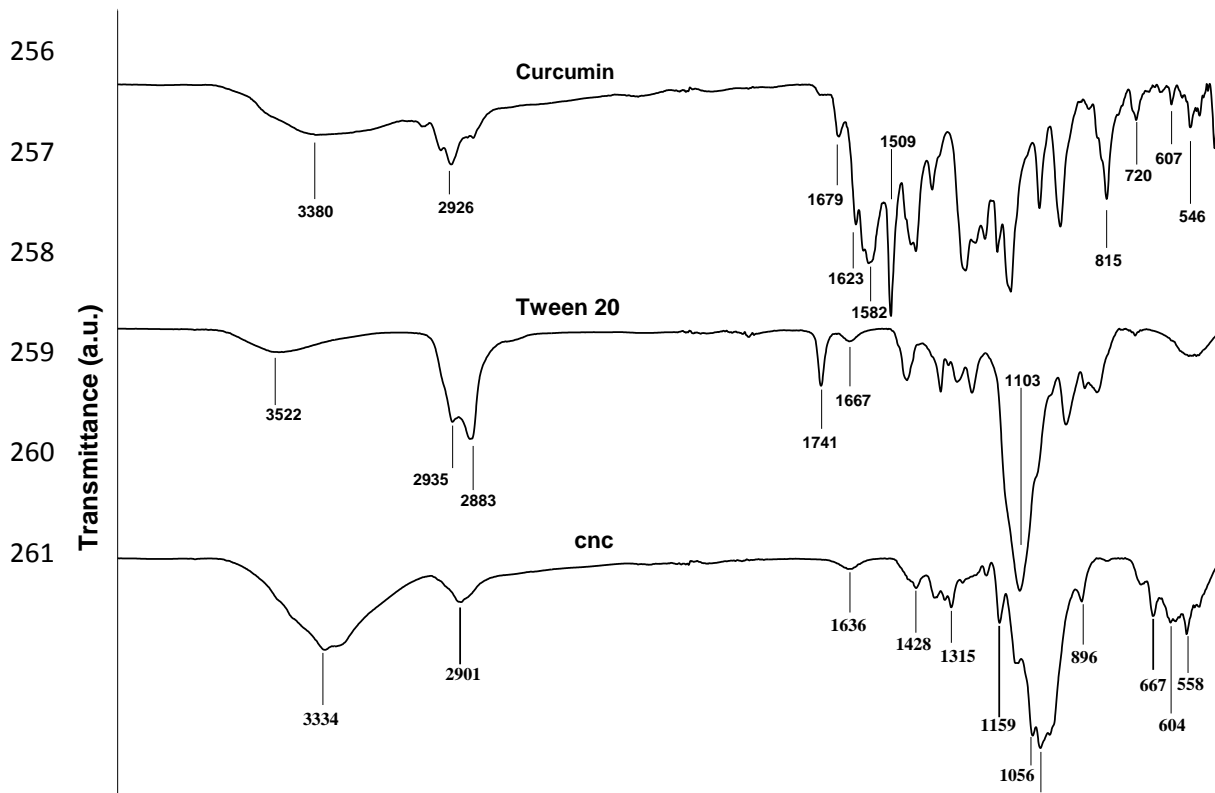


Fig. 1 FTIR spectra of curcumin, nonionic surfactant and nanocellulose (CNC)

From the FTIR spectrum of nanocellulose drug loaded in methanolic medium (curcumin/cnc/methanolic medium), it can be seen that the bands corresponding to the functional groups of CNC are more prominent (Fig. 2). However, small peaks at 1635cm^{-1} and 1595cm^{-1} are appeared due to the $\nu(\text{C}=\text{C})$ of the benzene ring, mixed $\nu(\text{C}=\text{C})$ and $\nu(\text{C}=\text{O})$ groups of curcumin (Bich et al. 2009; Mohan et al. 2012). Also in the FTIR spectrum of nanocellulose drug loaded in surfactant medium (curcumin/cnc/surfactant medium), the bands corresponding to the functional groups of CNC are prominent. In this spectrum a sharp peak appeared at 1652cm^{-1} which represents the carbonyl group from R-CO-O-R of Tween 20 (Ortiz-Tafoya and Tecante 2018). However, no new peak appeared in both spectrum of curcumin/cnc/methanolic medium and curcumin/cnc/surfactant medium.

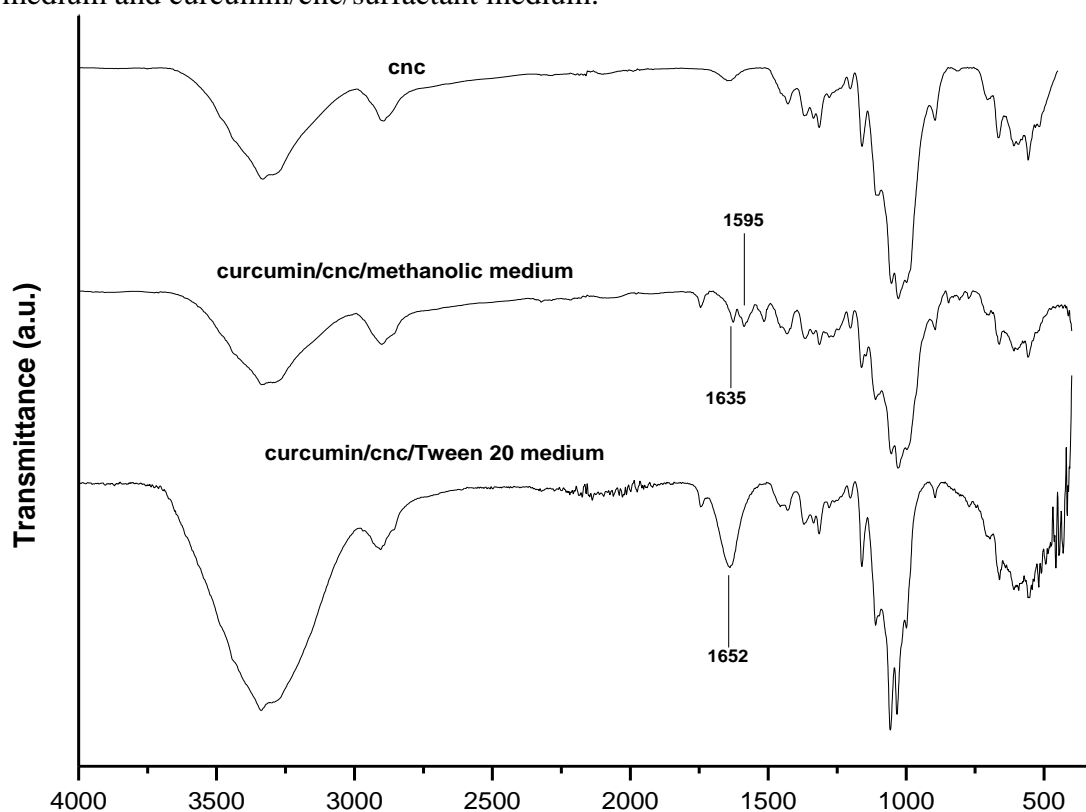


Fig. 2 FTIR spectra of cellulose nanoparticles, curcumin loaded cellulose nanoparticles in methanolic medium and curcumin loaded cellulose nanoparticles in **surfactant** medium

X-ray diffraction analysis

The X-ray diffraction (XRD) patterns of the curcumin, nanocellulose and curcumin incorporated nanocellulose were investigated via powder XRD analysis (Fig. 3). As shown in the diffractogram, the CNC exhibited peaks around $2\theta = 15^\circ, 16.5^\circ, 20.5^\circ, 22.5^\circ, 34.5^\circ$, which respectively represent the (1-10), (110), (102), (200), and (004) crystallographic planes of a typical cellulose I structure (Novo et al. 2015).

The diffraction pattern of curcumin exhibited peaks at angles $8.59^\circ, 11.24^\circ, 17.35^\circ, 18.19^\circ, 19.46^\circ, 21.28^\circ, 23.44^\circ, 24.58^\circ, 25.59^\circ, 26.17^\circ, 26.79^\circ, 27.39^\circ, 28.27^\circ, 28.97^\circ, 31.6^\circ$ and 36.23° which correspond to curcumin polymorph 1, indicating that curcumin sample exists as form 1 (Poornima et al. 2016; Sanphui et al. 2011). Curcumin exhibited well-defined sharp, narrow diffraction peaks between 10° and 30° , indicating the high crystalline structure (Cheng et al. 2017; Singh et al. 2014). The diffractogram of curcumin incorporated nanocellulose showed peaks which corresponded to both nanocellulose and curcumin. However, the peaks intensity of CNCs decreased after the incorporation of curcumin as shown in Fig. 3 which indicates a low crystallinity of the curcumin incorporated nanocellulose relative to the pure CNCs. From these results, it can be concluded that the interaction of the hydroxyl groups of CNCs with curcumin breaks the intermolecular and intramolecular hydrogen bonds of the CNCs and modifies the

crystalline regions of the CNCs. Therefore, the crystallinity of CNCs decreases by the interaction of curcumin with both the inner and surface hydroxyl groups.

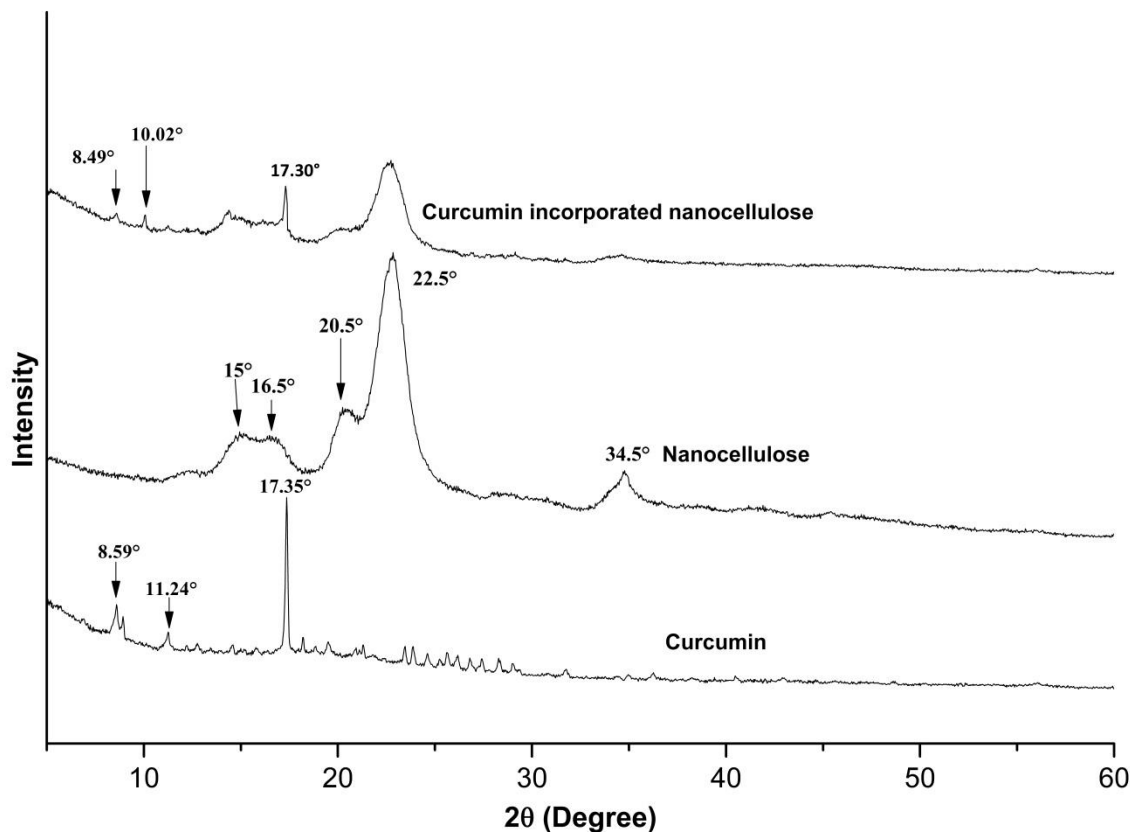


Fig. 3 X-ray diffraction (XRD) patterns of curcumin, nanocellulose and curcumin incorporated nanocellulose

Drug loading capacity

Since the solubility of curcumin in water is significantly low, we used nonionic surfactant (Tween 20) to dissolve the curcumin in aqueous medium. After that, the surfactant drug solution was stirred with cellulose nanocrystals to incorporate the drug into nanoparticles. (We used excess amount of curcumin, constant amount of nanocellulose with different concentration of

nonionic surfactant (0.8%,1.6%, 2.4%, 3.2%, 4%, 4.8%, 5.6% (w/v)) for the drug loading process. For the comparison of drug loading capacity, curcumin was incorporated into nanocellulose in methanolic medium. (Here, the same concentration of curcumin and same amount of nanocellulose were used as similar to those used in surfactant solutions). As shown in Fig. 4, the drug loading capacity of nanocellulose increased with increasing the surfactant concentration of the medium. It increased from 0.1mg/g to 7.73 mg/g with increasing the surfactant concentration from 0% to 4%. The highest drug loading capacity of nanocellulose was given at which the surfactant concentration showed the highest solubility of curcumin. After that, the loading capacity of nanocellulose was not increased with increasing the surfactant concentration. For curcumin dissolved in methanolic medium, the maximum drug loading capacity was 3.35 mg/g. It showed almost two fold increases in the drug loading capacity of nanocellulose in surfactant medium compared to methanolic medium. This may be due to the formation of micelles facilitating the incorporation of drug into nanoparticles.

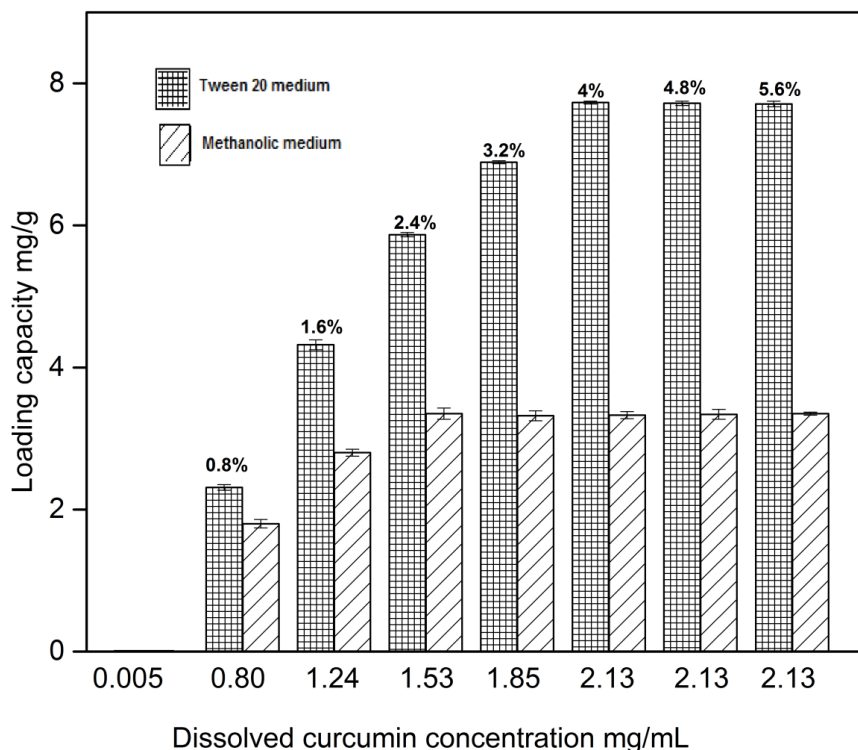


Fig. 4 Drug loading capacity of nanocellulose in surfactant and methanolic medium

Surfactant micelles are formed at the critical micelle concentration in aqueous medium due to the attainment of minimum free energy state. The critical micelle concentrations of nonionic surfactants are lower when compared to other ionic surfactants. Most micelles are spherical in shape and contain around 60-100 surfactant molecules. It has the hydrophobic oil-like core formed from the hydrocarbon chains surrounded by hydrophilic head groups of surfactant molecules. Formation of micelle facilitates the incorporation of poorly water-soluble drug in aqueous medium, which results in an increase in the apparent aqueous solubility of the drug. There are a number of possible locations of solubilization for a drug in a micelle, depending on their hydrophobicity.

As shown in Fig. 5a, hydrophilic drugs can be adsorbed on the surface of hydrophilic head region of the micelle. Drugs with intermediate solubility can be adsorbed between the hydrophilic head groups of surfactant micelle or in the palisade layer which is in between the hydrophilic and the first few carbon atoms of the hydrophobic tail (Fig. 5b,c). Drugs which are highly hydrophobic may be located in the inner core of the micelle. In this case, curcumin is highly hydrophobic and therefore, it may be adsorbed to the inner core of the micelle (Fig. 5d).

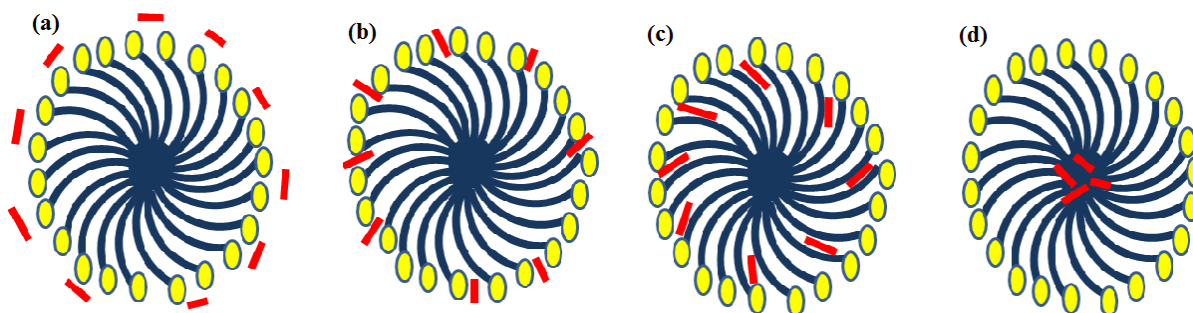
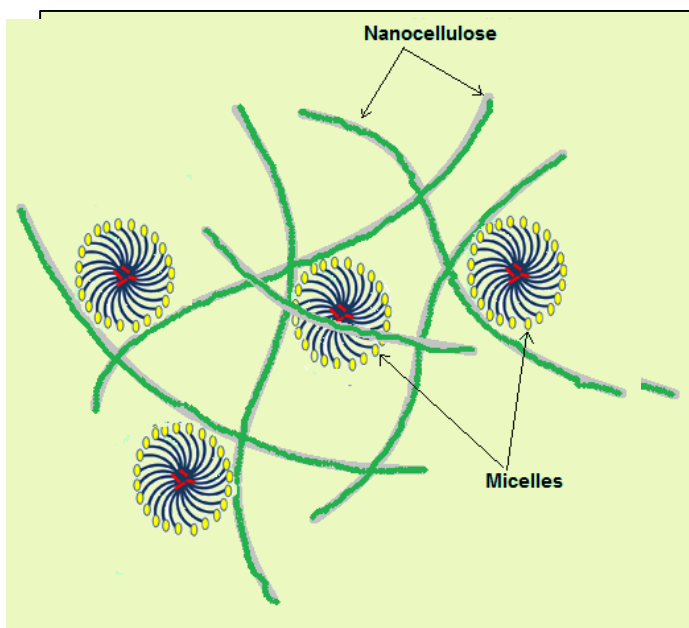


Fig. 5 Possible locations of drug in surfactant micelles, based on the drug hydrophobicity. The red bold lines represent the drug molecules, yellow circles display the surfactant heads and blue curved lines represents the hydrophobic tails of surfactants

Many researches have been discussed chemical strategies for surface modification of nanocelluloses. The main aspect to be considered here is that in contrast to complex chemical modification of cellulose, simple addition of surfactants is an appealing alternative. In such scenarios, physical adsorption such as charge–charge interactions, association of hydrophobic groups, and hydrogen bonding plays a key role in their association behavior. Adsorbing nonionic surfactants is a feasible method to enhance the compatibility of the hydrophilic cellulosic material with the typically hydrophobic materials. The hydrophilic groups of nonionic surfactants may have affinity for adsorption to the cellulose due to the hydroxyl groups of cellulose (as shown in Fig. 6). However, not all the hydroxyl groups present in cellulose nanocrystals are accessible. This is because some of them are oriented towards the inner part of nanoparticle. Previous literature reported that only one half of hydroxyl groups present in cellulose chains of nanoparticle are reactive (Ching et al. 2006). It also reported that the primary hydroxyl on C6 is most reactive (Gan et al. 2017).



387

388 **Fig. 6** Possible interactions of surfactant micelles with nanocellulose

389 From previous studies, different types of surfactants have been used to improve the release of
390 drugs in different types of drug delivery systems. Pandav et al. (2013) reported that the
391 encapsulation efficiency of microparticulate drug delivery system of propranolol
392 hydrochloride was directly proportional to surfactant concentration. Furthermore, Tween 80 was
393 shown to be the more effective surfactant as compared to Span 60 for loading of curcumin onto
394 starch nanoparticles (Chin et al. 2014). In our previous study, we observed that the encapsulation
395 efficiency of curcumin in chitosan hydrogel decreased with increasing the **surfactant**
396 concentration. This was due to the fact that the higher concentration of the emulsifier increases
397 the partition of the drug from internal to external phase due to the increased solubility of the drug
398 in the external phase. But, in this study, the loading capacity of nanocellulose for curcumin
399 increased with increasing the **surfactant** concentration. This is due to the increase of the number
400 of micelle formation and hence, facilitating the incorporation of drug into nanocellulose
401 particles.

402 *Drug release*

403 Drug release studies were carried out in simulated gastric fluid (SGF) and phosphate buffered
404 saline (PBS) solution. Constant weight of nanoparticles which adsorbed highest amount of
405 curcumin in methanolic medium and Tween 20 medium were selected for drug release studies.
406 All the nanoparticles showed initial burst release during first 30 min due to the fraction of drug
407 which is weakly bound to the large surface area of nanoparticles. As shown in Fig. 7 and Fig. 8,
408 among all the nanoparticles, the highest drug release shown by the nanoparticles drug loaded

insurfactant medium (TW/CNC), compared to the nanoparticles drug loaded in methanolic medium (METH/CNC).The nanoparticles drug loaded in **surfactant** medium reached to equilibrium drug release stage at around 270 minutes (in SGF medium) and 350 minutes (in PBS medium) while the nanoparticles drug loaded in methanolic medium reached to that stage at around 150 minutes and 270 minutes in SGFand PBS medium respectively. The nanoparticles drug loaded in both **surfactant** and methanolic medium showed lower drug release in PBS medium. The reason for this may be due to the less stability of curcumin in neutral or pHs above neutral. In addition, previous studies indicated that the stability of curcumin can be strongly improved by lowering the pH of the medium (Khalkhali et al. 2015; Rao and Rao 2011; Wang et al. 1997).

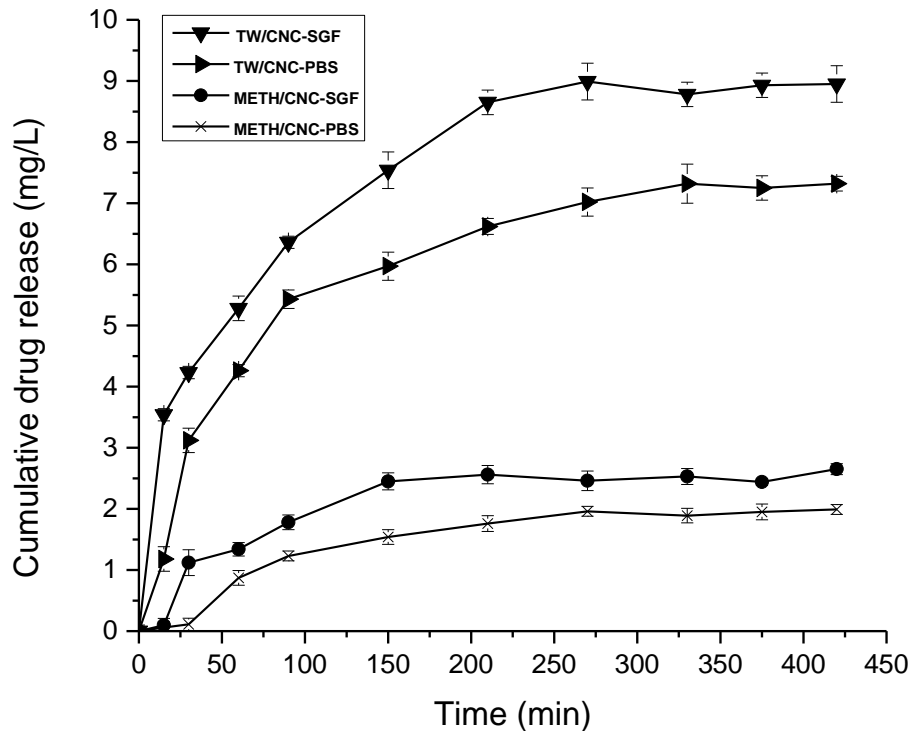


Fig. 7 Drug release from cellulose nanoparticles (TW/CNC and METH/CNC) to SGF and PBS media

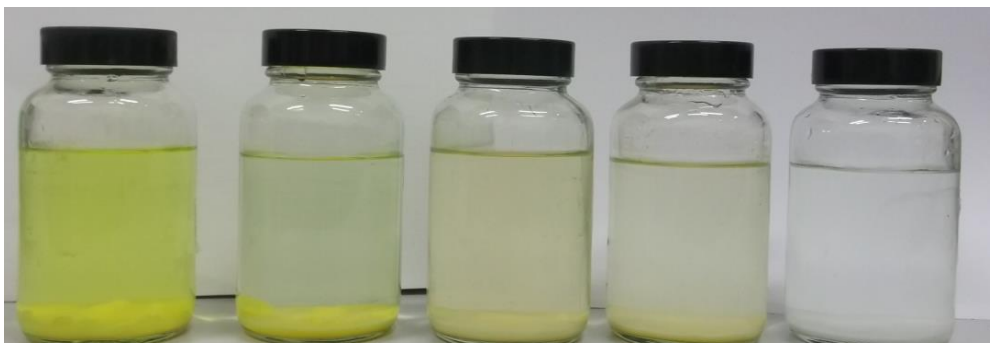


Fig. 8 Drug release from: **a** W/CNC into SGF medium; **b** METH/CNC into SGF medium; **c** TW/CNC into PBS medium; **d** METH/CNC into PBS medium and control

According to our previous study, the nanoparticles prepared by sulphuric acid hydrolysis method were within the range of 200–300 nm in length and 40–50 nm in width (Sampath et al. 2017). As the particle size gets smaller, their surface area to volume ratio gets larger. This would imply that more of the drug is closer to the surface of the nanoparticle compared to a larger molecule. Being at or near the surface would lead to faster drug release (Rizvi and Saleh 2017). Average gastric emptying times for healthy individuals at 1, 2, and 4 h are >90%, 60% and 10%, respectively (Jobe et al. 2013). Due to the highest drug release shown in SGF medium, and faster drug release, these drug delivery systems are more suitable for stomach delivery of curcumin. The higher drug release by TW/CNC-SGF and TW/CNC-PBS nanoparticles, which immersed in SGF and PBS media, is due to the presence of adsorbed nonionic surfactants into the nanoparticles. These surfactants facilitate the dispersion of curcumin in aqueous medium. They improve the solubility of poorly water soluble curcumin by formation of micelles and adsorbing the hydrophobic drug into the core of the micelle structure. Hydrophilic head groups show more affinity towards aqueous medium and thereby improve the solubility of the drug in SGF and PBS medium. In contrast, for METH/CNC-SGF and METH/CNC-PBS conditions, the interactions between nanocellulose and curcumin molecules are most probably by hydrogen bonds. Since, there is no micelle formation or facilitation for the dispersion of this poorly water soluble drug,

the release amount of drug to the SGF and PBS medium is very low compared to TW/CNC-SGF and TW/CNC-PBS conditions.

Similar drug delivery systems are also reported with enhanced solubility of curcumin using Tween 20. The drug delivery studies on chitin beads incorporated with curcumin, carried out by Ratanajajaroen and Ohshima (2012) reported that the solubility of curcumin increased up to 0.767 mg/mL with the presence of 2% (v/v) Tween 20 in acetate buffer medium (pH 5.5). They also found that the drug release rate from chitin beads was proportional to the surfactant concentration. Furthermore, the drug delivery studies on submicrometer spray-dried chitosan/Tween 20 particles by O'Toole et al. (2012) showed that the curcumin can be completely release from the matrix in both phosphate buffered saline solution and 1% acetic acid over a 2 h period. In addition, it showed 12.7-fold increase in curcumin solubility with 0.05 w/v% of surfactant in 1% acetic acid solution. From our previous study of curcumin delivery using chitosan/nanocellulose/surfactant hydrogel, we achieved 3.98mg/L of curcumin release in SGF medium after 7.5h. In this study, we achieved 8.99 mg/L of curcumin release in SGF medium at around 270 minutes. Therefore, these curcumin loaded cellulose nanoparticles provide more effective approach for delivery of curcumin to stomach and upper intestinal tract.

Drug activity

The drugs are often inevitable and therefore, the chemical reactivity related to biological activity of the drug is most important parameter to be concerned when selecting a drug delivery carrier. For some drug delivery systems, drugs deteriorate due to the destructive interactions with the carrier molecules. In order to prevent this, the carrier should be prone to destructive interactions with the drug and able to be delivered into the body without any chemical deterioration. The UV-

473 Vis spectra of pure drug and released drug can be used to determine if any deterioration reaction
474 happened due to the destructive interactions between drug and carrier molecules (Bashir et al.
475 2016). Curcumin has three reactive functional groups, namely one diketone moiety, and two
476 phenolic groups which associated with its different biological activities. The diketone moiety
477 involves in nucleophilic addition reactions and C-4 participates in hydrogen donation reactions
478 leading to oxidation of curcumin; which are most important chemical reactions associated with
479 its biological activities (Ahmed et al. 2017).

480 As shown in Fig.9a, UV-Vis spectrum of pure curcumin shows an absorption peak around 427
481 nm, which can be assigned to the low-energy π - π^* excitation of the chromophore, that formed
482 due to the enolization of the diketone group and conjugation between the π -electron clouds of the
483 two vinylguaiacol (Zsila et al. 2004). In this study, curcumin is in contact with nonionic
484 surfactant, cellulose, simulated gastric fluid and phosphate buffer saline solution. Fig. 9b
485 represents the UV-Vis spectra of curcumin, which is released from nanocellulose (drug loaded in
486 surfactant medium) into simulated gastric medium and phosphate buffered saline solution. It is
487 clear that the absorption maximum of both these spectra is around 427 nm. It remains unchanged
488 without shifting upward or downward regions of the spectrum. Fig. 9c represents the UV-Vis
489 spectra of curcumin, which is released from nanocellulose (drug loaded in methanolic medium)
490 into simulated gastric medium and phosphate buffered saline solution. Since the released amount
491 of drug from these nanoparticles is very low, the absorption peak around 427 nm is slightly small
492 compared to the absorption maximum of Fig. 9b. However, in this situation the absorption
493 maximum (427 nm) also remain unchanged (without shifting upward or downward direction of
494 the spectrum). Therefore, it revealed that the reactive functional groups, which are associated

with the biological activity of curcumin retained without any deterioration due to any denaturation reaction with drug containing media or with carrier molecules (nanocellulose).

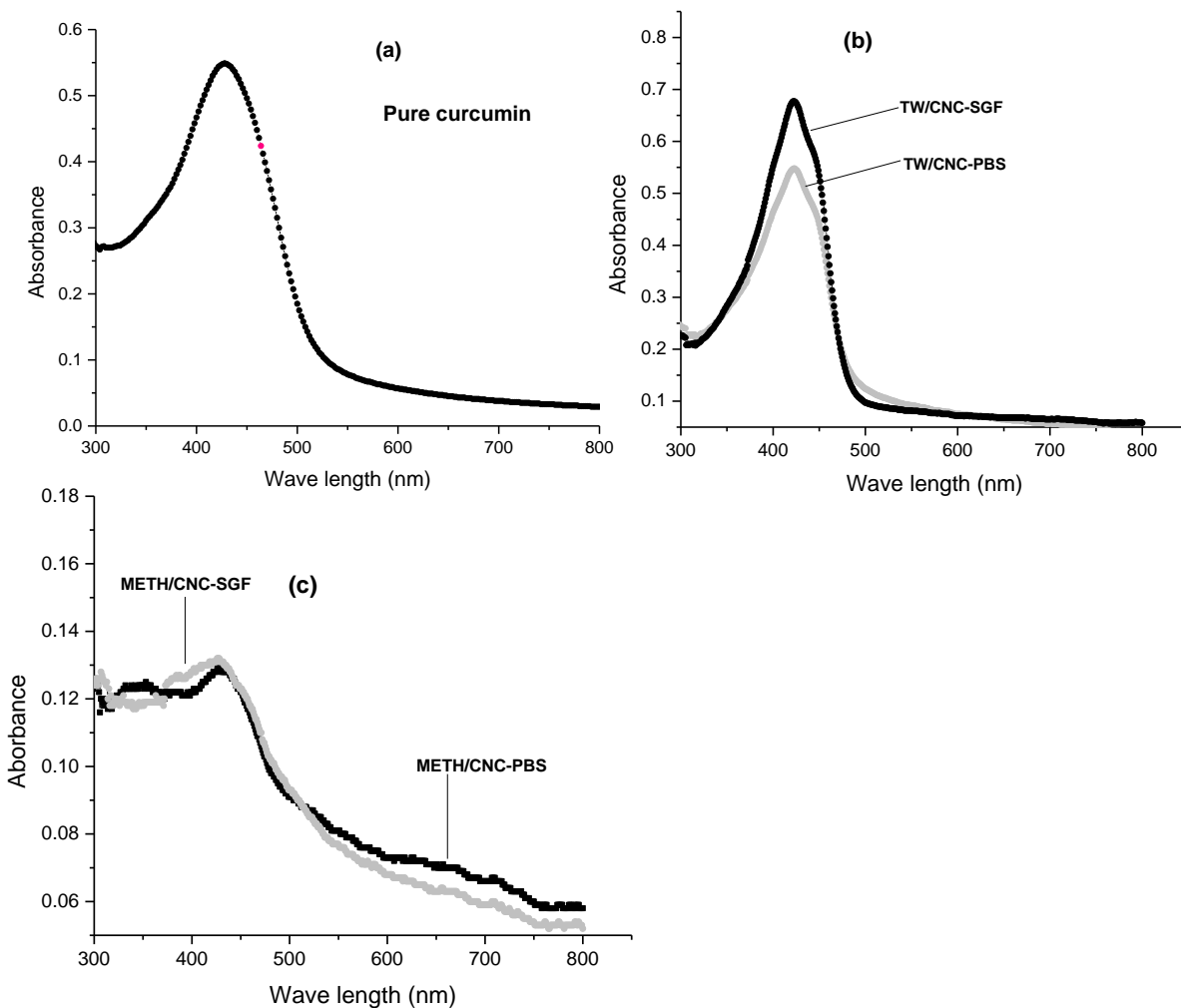


Fig. 9 UV-Vis spectra of: **a** pure curcumin; curcumin release from TW/CNC into PBS and SGF media; **c** curcumin release from METH/CNC into PBS and SGF media

Solubility studies

For the encapsulation of curcumin into nanocellulose, the curcumin was dissolved in distilled water medium. Therefore, the solubility studies of curcumin were carried out in distilled water with the presence of nonionic surfactant at 37° C. As shown in Fig. 10 the dissolution rate of curcumin increased with increasing the surfactant concentration in dissolution medium and the maximum dissolution of curcumin was 2.13 mg/mL in distilled water containing 4% w/v of surfactant. Addition of surfactant to the distilled water improves the dissolution of pure drug by facilitating the dispersion of drug by micelle solubilization in the bulk medium. The amount of surfactant needed depends on the critical micelle concentration and the solubilization capacity for curcumin in surfactant micelles. It may be the reason for the fact that the amount of dissolved curcumin did not increase above 4% of surfactant in distilled water. It reached a minimum surface tension at 4% of surfactant with no significant change at higher concentrations. Similar results were obtained from the studies on solubility of curcumin in aqueous polysorbate micelle, by Inchai et al. (2015). Their studies showed that the solubility of curcumin increased up to 2.7 mg/mL in 20% aqueous solution of Tween 20. From our previous study, we achieved the solubility of curcumin with an upper limit of 3.014 ± 0.041 mg/mL in the presence of 3.2% (w/v) Tween 20 in simulated gastric medium. This may be due to the higher stability of curcumin in acidic medium compared to neutral or alkaline medium. Previous studies have also confirmed that the aqueous solubility and the stability of curcumin is higher in acidic medium compared to neutral or higher pH values (Khalkhali et al. 2015; Wang et al. 1997).

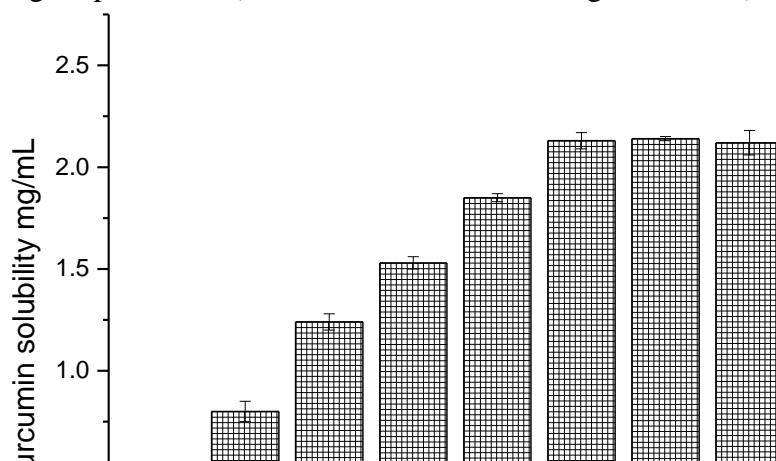


Fig. 10 Solubility of curcumin in distilled water with different concentrations of nonionic surfactant

Conclusion

Cellulose nanocrystals were synthesized using microcrystalline cellulose via sulphuric acid hydrolysis method. Curcumin was extracted using dried rhizomes of *Curcuma longa* following the methanolic extraction method. The incorporation of drug and surfactant into the cellulose nanoparticles was verified through the FTIR characterization. The drug loading capacity of nanocellulose increased from 0.1 mg/g to 7.73 mg/g with increasing the surfactant concentration from 0% to 4%. This may be due to the formation of micelles facilitating the incorporation of drug into nanoparticles. The maximum drug loading capacity of nanocellulose in methanolic medium was 3.35 mg/g. Among all the nanoparticles, the highest drug release shown by the nanoparticles drug loaded in surfactant medium (TW/CNC) compared to the nanoparticles drug loaded in methanolic medium (METH/CNC). The nanoparticles drug loaded in both surfactant and methanolic medium showed lower drug release in PBS medium due to the less stability of curcumin in neutral or pHs above neutral. Solubility of curcumin increased with an upper limit of 2.13 mg/mL with the presence of 4% (w/v) surfactant in distilled water. In addition, curcumin retained its structural integrity after release to the SGF and PBS media, which is a critical

requirement for preserving drug activity. In conclusion, the enhancement of bioavailability of curcumin using curcumin/nonionic surfactant-incorporated cellulose nanoparticles would represent an important step forward in nanopharmaceutical field.

Acknowledgments

The authors would like to acknowledge the financial support from the Ministry of Education of Malaysia FRGS-FP053-2015A and PRGS-PR005-2017A and University of Malaya PG160-2016A, ST017-2018, GPF 033A-2018, RU018I-2016 and International Funding AUA Scholars IF025-2018 for the success of this project.

References

- Ahmed M, Qadir MA, Shafiq MI, Muddassar M, Hameed A, Arshad MN, Asiri AM (2017) Curcumin: Synthesis optimization and in silico interaction with cyclin dependent kinase. *Acta Pharmaceut* 67:385-395
- Bashir S, Teo YY, Ramesh S, Ramesh K (2016) Synthesis, characterization, properties of N-succinyl chitosan-g-poly (methacrylic acid) hydrogels and in vitro release of theophylline. *Polymer* 92:36-49
- Bich VT, Thuy NT, Binh NT, Huong NTM, Yen PND, Luong TT (2009) Structural and spectral properties of curcumin and metal-curcumin complex derived from turmeric (*Curcuma longa*). In: Cat DT, Pucci A, Wandelt K (eds) *Physics and engineering of new materials. Springer proceedings in physics*. Springer, Berlin, pp 271-278
- Chaudhari SP, Dugar RP (2017) Application of surfactants in solid dispersion technology for improving solubility of poorly water soluble drugs. *J Drug Deliv Sci Tec* 41:68-77
- Cheng C, Peng S, Li Z, Zou L, Liu W, Liu C (2017) Improved bioavailability of curcumin in liposomes prepared using a pH-driven, organic solvent-free, easily scalable process. *Rsc Adv* 7:25978-25986
- Chin SF, Yazid M, Akmar SN, Pang SC (2014) Preparation and characterization of starch nanoparticles for controlled release of curcumin. *Int J Polym Sci* 2014:340121
- Ching YC, Md. Ershad MA, Luqman CA, Choo KW, Yong C K, Sabariah JJ, Chuah CH, Liou NS (2016) Rheological properties of cellulose nanocrystal-embedded polymer composites: a review. *Cellulose* 23:1011-1030.
- Ching YC and Ng TS (2014). Effect of preparation conditions on cellulose from oil palm empty fruit bunch fiber. *Bioresource* 9(4): 6373- 6385
- de Castro DO, Tabary N, Martel B, Gandini A, Belgacem N, Bras J (2018) Controlled release of carvacrol and curcumin: bio-based food packaging by synergism action of TEMPO-oxidized cellulose nanocrystals and cyclodextrin. *Cellulose* 25:1249-1263

- De R, Kundu P, Swarnakar S, Ramamurthy T, Chowdhury A, Nair GB, Mukhopadhyay AK (2009) Antimicrobial activity of curcumin against *Helicobacter pylori* isolates from India and during infections in mice. *Antimicrob Agents Ch* 53:1592-1597
- Fugita RA, Gálico DA, Guerra RB, Perpétuo GL, Treu-Filho O, Galhiane MS, Mendes RA, Bannach G (2012) Thermal behaviour of curcumin. *Braz J Therm Anal* 1:19-23
- Gan S, Zakaria S, Chia CH, Chen RS, Ellis AV, Kaco H (2017) Highly porous regenerated cellulose hydrogel and aerogel prepared from hydrothermal synthesized cellulose carbamate. *PLoS One* 12:e0173743
- Gunathilake TMSU, Ching YC, Chuah CH (2017) Enhancement of curcumin bioavailability using nanocellulose reinforced chitosan hydrogel. *Polymers* 9:64
- Gunathilake TMSU, Ching YC, Chuah CH, Illias HA, Ching KY, Singh R, Nai-Shang L (2018) Influence of a nonionic surfactant on curcumin delivery of nanocellulose reinforced chitosan hydrogel. *Int J Biol Macromol* 118:1055-1064
- Gunathilake T M SU, Ching YC, Kuan YC, Chuah CH and Luqman CH (2017) Biomedical and microbiological applications of bio-based porous materials: a review. *Polymer*, 9: 160. doi:10.3390/polym9050160
- Gustafson HH, Holt-Casper D, Grainger DW, Ghandehari H (2015) Nanoparticle uptake: the phagocyte problem. *Nano today* 10:487-510
- Ibrahim S, Tagami T, Kishi T, Ozeki T (2018) Curcumin marinosomes as promising nano-drug delivery system for lung cancer. *Int J Pharmaceut* 540:40-49
- Inchai N, Ezure Y, Hongwiset D, Yotsawimonwat S (2015) Investigation on solubility and stability of curcumin in aqueous polysorbate micelle. *International Journal of Management and Applied Science* 3:157-161
- Jankun J, Wyganowska-Świątkowska M, Dettlaff K, Jelińska A, Surdacka A, Wątróbska-Świetlikowska D, Skrzypczak-Jankun E (2016) Determining whether curcumin degradation/condensation is actually bioactivation. *Int J Mol Med* 37:1151-1158
- Jobe BA, Richter JE, Hoppo T, Peters JH, Bell R, Dengler WC, DeVault K, Fass R, Gyawali CP, Kahrilas PJ, Lacy BE, Pandolfino JE, Patti MG, Swanstrom LL, Kurian AA, Vela MF, Vaezi M, DeMeester TR (2013) Preoperative diagnostic workup before antireflux surgery: An evidence and experience-based consensus of the esophageal diagnostic advisory panel. *J Am Coll Surgeons* 217:586-597
- Kamaraj S, Palanisamy UM, Mohamed MSBK, Gangasalam A, Maria GA, Kandasamy R (2018) Curcumin drug delivery by vanillin-chitosan coated with calcium ferrite hybrid nanoparticles as carrier. *Eur J Pharm Sci* 116:48-60
- Khalkhali M, Sadighian S, Rostamizadeh K, Khoeini F, Naghibi M, Bayat N, Habibizadeh M, Hamidi M (2015) Synthesis and characterization of dextran coated magnetite nanoparticles for diagnostics and therapy. *Bioimpacts* 5:141
- Kolev TM, Velcheva EA, Stamboliyska BA, Spiteller M (2005) DFT and experimental studies of the structure and vibrational spectra of curcumin. *Int J Quantum Chem* 102:1069-1079
- Löbmann K, Svagan AJ (2017) Cellulose nanofibers as excipient for the delivery of poorly soluble drugs. *Int J Pharmaceut* 533:285-297
- Mohan PK, Sreelakshmi G, Muraleedharan C, Joseph R (2012) Water soluble complexes of curcumin with cyclodextrins: Characterization by FT-Raman spectroscopy. *Vib Spectrosc* 62:77-84

- Yallapu MM, Dobberpuhl MR, Maher DM, Jaggi M, Chauhan SC (2012) Design of curcumin loaded cellulose nanoparticles for prostate cancer. *Curr Drug Metab* 13:120-128
- Novo LP, Bras J, García A, Belgacem N, Curvelo AA (2015) Subcritical water: a method for green production of cellulose nanocrystals. *ACS Sustain Chem Eng* 3:2839-2846
- Ntoutoume GMAN, Granet R, Mbakidi JP, Brégier F, Léger DY, Fidanzi-Dugas C, Lequart V, Joly N, Liagre B, Chaleix V, Sol V (2016) Development of curcumin–cyclodextrin/cellulose nanocrystals complexes: new anticancer drug delivery systems. *Bioorg Med Chem Lett* 26:941-945
- O'Toole MG, Henderson RM, Soucy PA, Fasciotto BH, Hoblitzell PJ, Keynton RS, Ehringer WD, Gobin AS (2012) Curcumin encapsulation in submicrometer spray-dried chitosan/Tween 20 particles. *Biomacromolecules* 13:2309-2314
- Ortiz-Tafoya M, Tecante A (2018) Physicochemical characterization of sodium stearyl lactylate (SSL), polyoxyethylene sorbitan monolaurate (Tween 20) and κ -carrageenan. *Data Brief* 19:642-650
- Pandav S, Lokhande A, Naik J (2013) Assessment of microparticulate drug delivery system of propranolol hydrochloride prepared by multiple solvent emulsion technique. *Int J Pharm Pharm Sci* 5:831-835
- Phanthong P, Ma Y, Guan G, Abudula A (2015) Extraction of nanocellulose from raw apple stem. *Journal of the Japan Institute of Energy* 94:787-793
- Poornima B, Prasad K, Bharathi K (2016) Evaluation of solid-state forms of curcuminoids. *Int J Pharm Sci Res* 7:4035
- Rangel-Yagui CO, Pessoa Jr A, Tavares LC (2005) Micellar solubilization of drugs. *J Pharm Pharm Sci* 8:147-163
- Rao JV, Rao M (2011) Increased solubility and stability of curcumin in lactic acid. *Int J Pharm Bio Sci* 1:50-53
- Ratanajiaroen P, Ohshima M (2012) Synthesis, release ability and bioactivity evaluation of chitin beads incorporated with curcumin for drug delivery applications. *J Microencapsul* 29:549-558
- Rizvi SA, Saleh AM (2017) Applications of nanoparticle systems in drug delivery technology. *Saudi Pharm J* 26(1): 64–70
- Sadeghifar H, Filpponen I, Clarke SP, Brougham DF, Argyropoulos DS (2011) Production of cellulose nanocrystals using hydrobromic acid and click reactions on their surface. *J Mater Sci* 46:7344-7355
- Sahlin K, Forsgren L, Moberg T, Bernin D, Rigdahl M, Westman G (2018) Surface treatment of cellulose nanocrystals (CNC): effects on dispersion rheology. *Cellulose* 25:331-345
- Sampath UTM, Ching YC, Chuah CH, Singh R, Lin PC (2017) Preparation and characterization of nanocellulose reinforced semi-interpenetrating polymer network of chitosan hydrogel. *Cellulose* 24:2215-2228
- Sanphui P, Goud NR, Khandavilli UR, Bhanoth S, Nangia A (2011) New polymorphs of curcumin. *Chem Commun* 47:5013-5015
- Santos AM, Lopes T, Oleastro M, Pereira T, Alves CC, Seixas E, Chaves P, Machado J, Guerreiro AS (2018) Cyclooxygenase inhibition with curcumin in *Helicobacter pylori* infection. *Nutrire* 43:7
- Singh PK, Wani K, Kaul-Ghanekar R, Prabhune A, Ogale S (2014) From micron to nano-curcumin by sophorolipid co-processing: highly enhanced bioavailability, fluorescence, and anti-cancer efficacy. *Rsc Adv* 4:60334-60341

685 Wang YJ, Pan MH, Cheng AL, Lin LI, Ho YS, Hsieh CY, Lin JK (1997) Stability of curcumin
686 in buffer solutions and characterization of its degradation products. J Pharmaceut Biomed
687 15:1867-1876
688 Zsila F, Bikádi Z, Simonyi M (2004) Circular dichroism spectroscopic studies reveal pH
689 dependent binding of curcumin in the minor groove of natural and synthetic nucleic
690 acids. Org Biomol Chem 2:2902-2910

691

692 **List of figures**

693 **Fig. 1** FTIR spectra of curcumin, nonionic surfactant and nanocellulose (CNC)

694 **Fig. 2** FTIR spectra of cellulose nanoparticles, curcumin loaded cellulose nanoparticles in
695 methanolic medium and curcumin loaded cellulose nanoparticles in surfactant medium

696 **Fig. 3** X-ray diffraction (XRD) patterns of curcumin, nanocellulose and curcumin incorporated
697 nanocellulose

698 **Fig. 4** Drug loading capacity of nanocellulose in surfactant and methanolic medium

699 **Fig. 5** Possible locations of drug in surfactant micelles based on the drug hydrophobicity. The
700 red bold lines represent the drug molecules, yellow circles display the surfactant heads and blue
701 curved lines represents the hydrophobic tails of surfactants

702 **Fig. 6** Possible interactions of surfactant micelles with nanocellulose

703 **Fig. 7** Drug release from cellulose nanoparticles (TW/CNC and METH/CNC) to SGF and PBS
704 media

705 **Fig. 8** Drug release from: **a** TW/CNC into SGF medium; **b** METH/CNC into SGF medium; **c**
706 TW/CNC into PBS medium; **d** METH/CNC into PBS medium and **e** control

707 **Fig. 9** UV-Vis spectra of: **a** pure curcumin; **b** curcumin release from TW/CNC into PBS and
708 SGF media; **c** curcumin release from METH/CNC into PBS and SGF media

709 **Fig. 10** Solubility of curcumin in distilled water with different concentrations of nonionic
710 surfactant

711 **List of Tables**

712 **Table 1** Types of nanocellulose used for the drug release studies (based on the drug loading and
713 releasing medium)

714

715

716

717

718

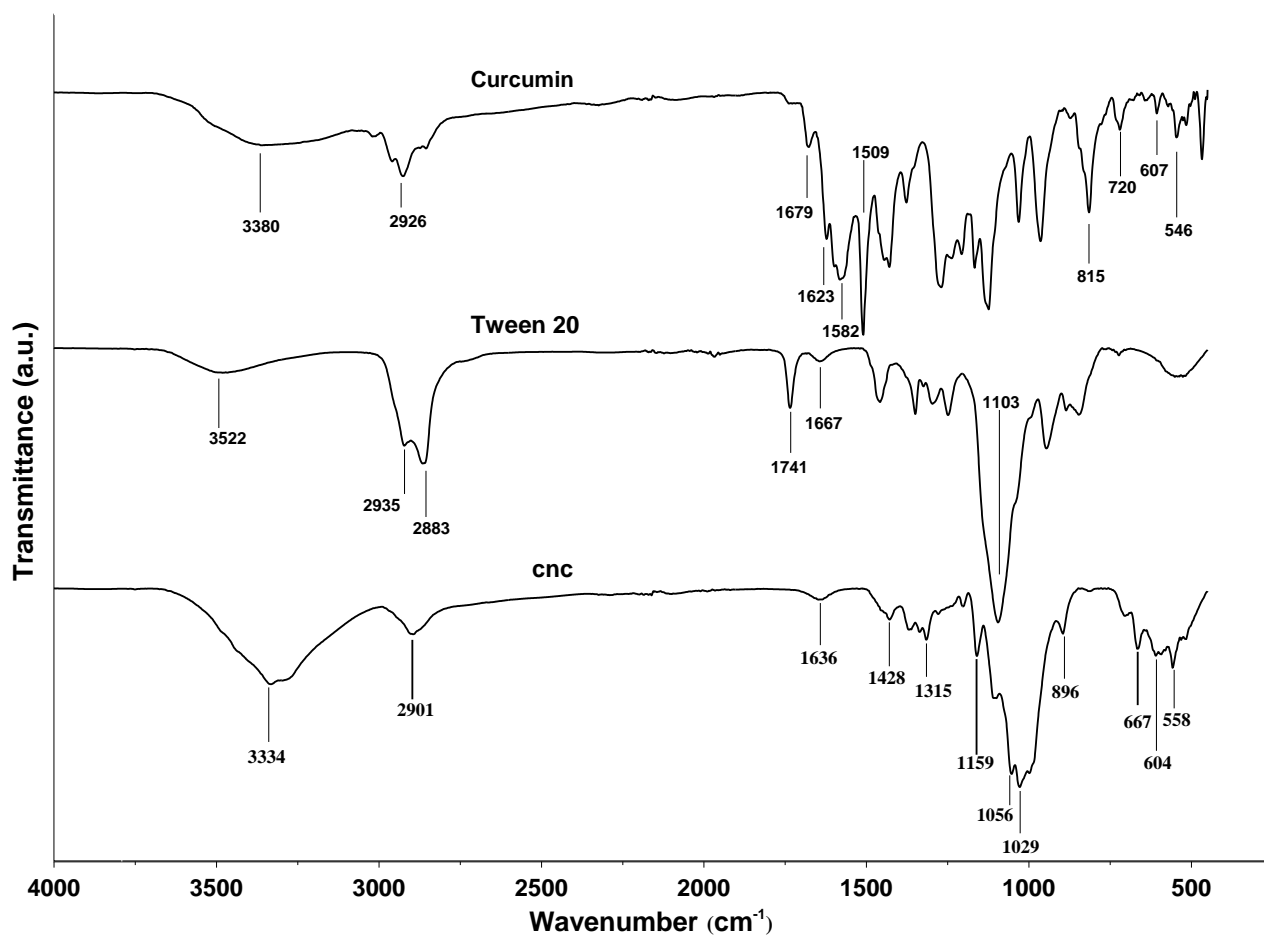


Fig. 1 FTIR spectra of curcumin, nonionic surfactant and nanocellulose (CNC)

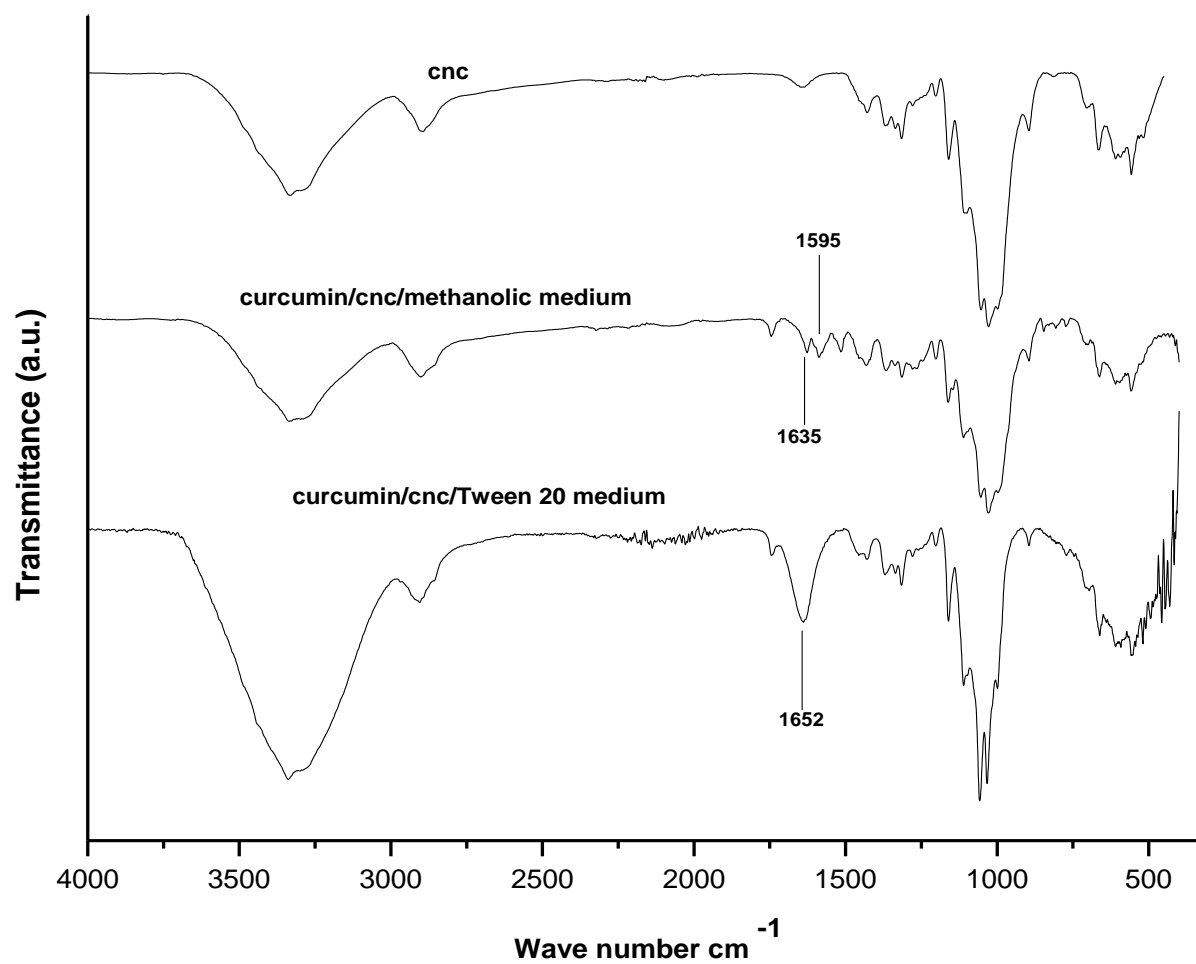


Fig. 2 FTIR spectra of cellulose nanoparticles, curcumin loaded cellulose nanoparticles in methanolic medium and curcumin loaded cellulose nanoparticles in surfactant medium

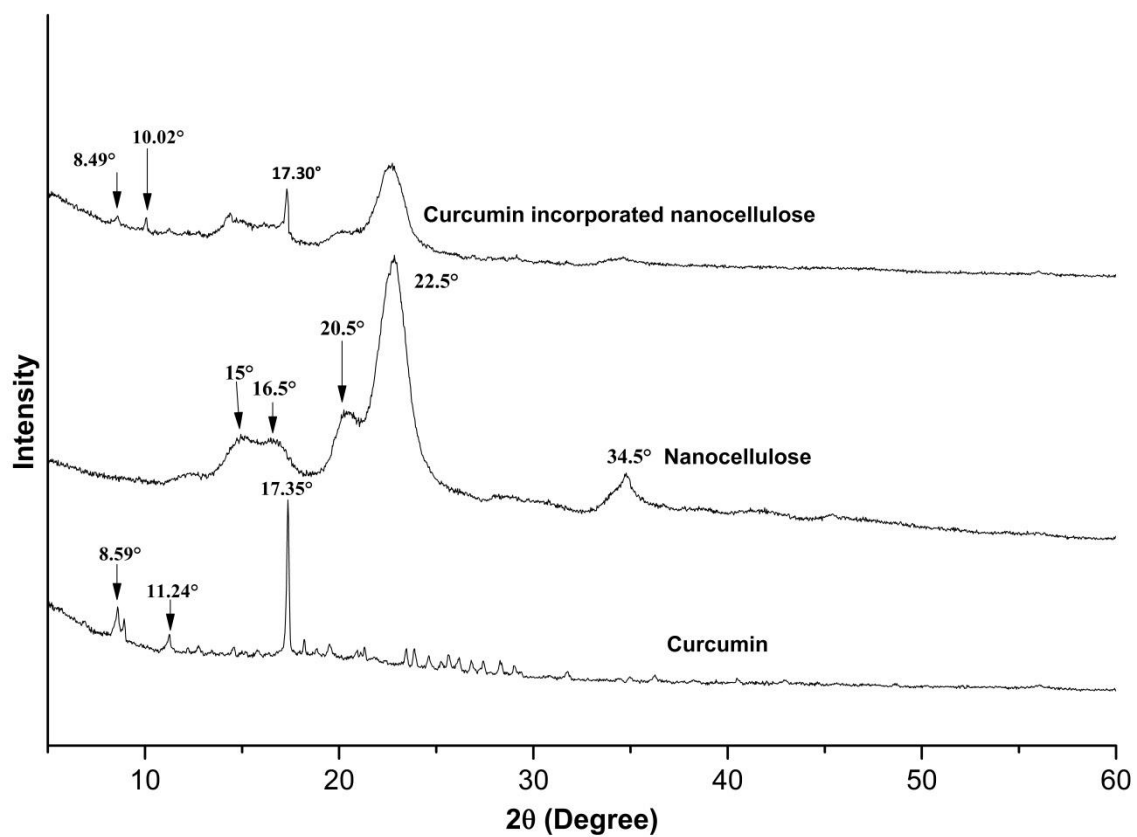


Fig. 3 X-ray diffraction (XRD) patterns of curcumin, nanocellulose and curcumin incorporated nanocellulose

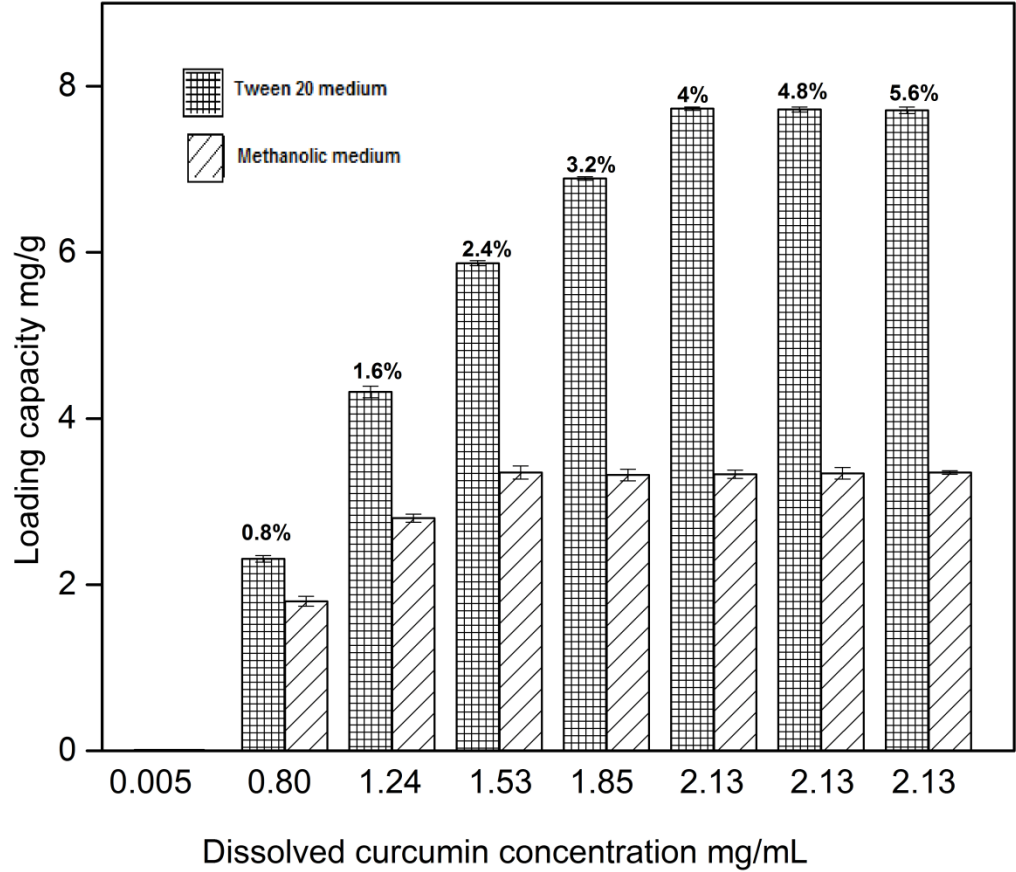


Fig. 4 Drug loading capacity of nanocellulose in surfactant and methanolic medium

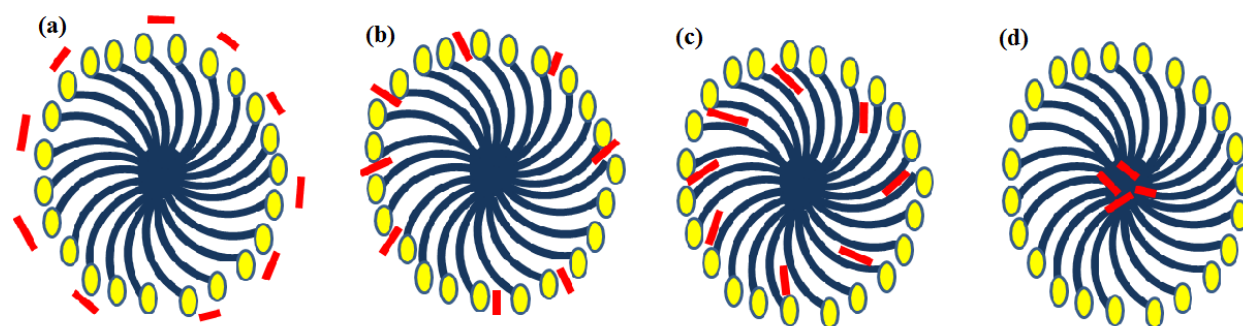


Fig. 5 Possible locations of drug in surfactant micelles, based on the drug hydrophobicity. The red bold lines represent the drug molecules, yellow circles display the surfactant heads and blue curved lines represents the hydrophobic tails of surfactants

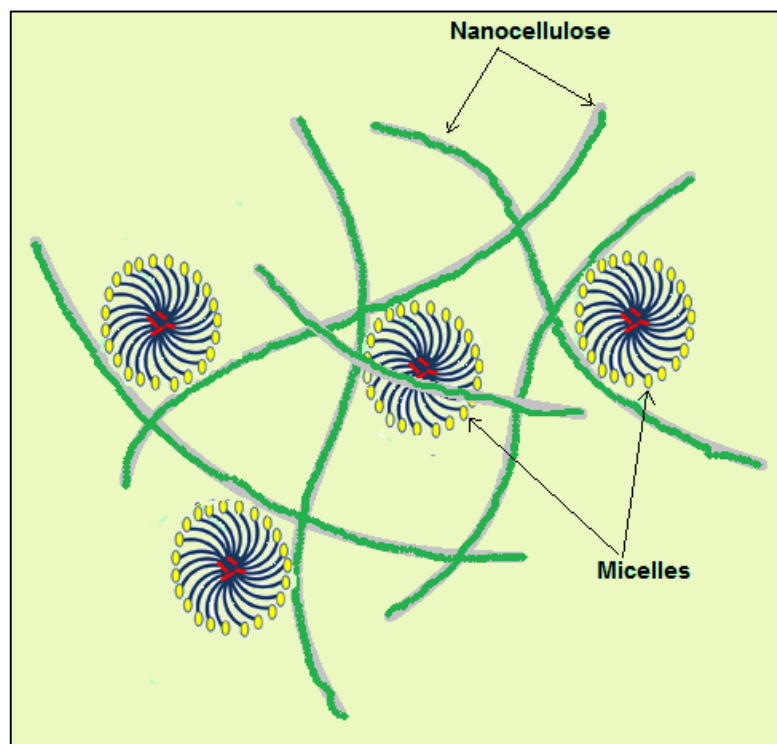


Fig. 6 Possible interactions of surfactant micelles with nanocellulose

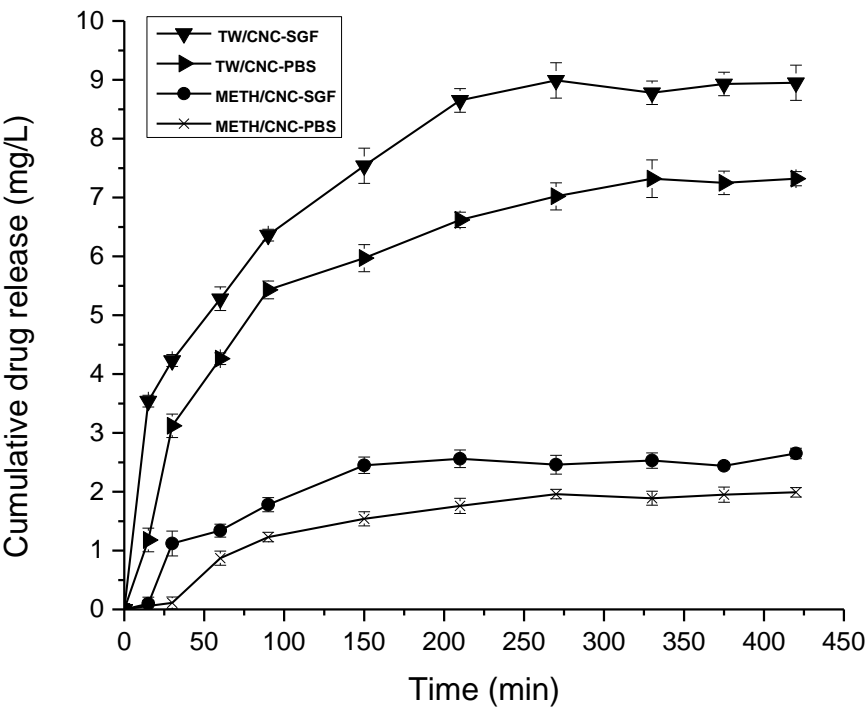


Fig. 7 Drug release from cellulose nanoparticles (TW/CNC and METH/CNC) to SGF and PBS media

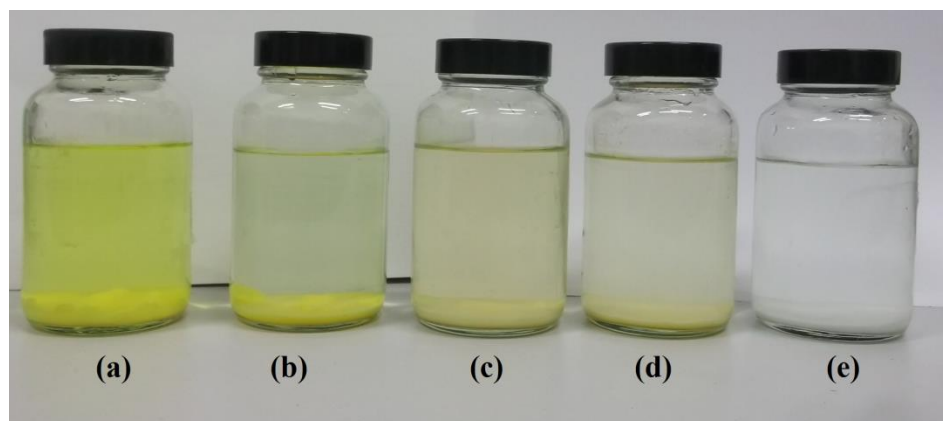


Fig. 8 Drug release from: **a** TW/CNC into SGF medium; **b** METH/CNC into SGF medium; **c** TW/CNC into PBS medium; **d** METH/CNC into PBS medium and **e** control

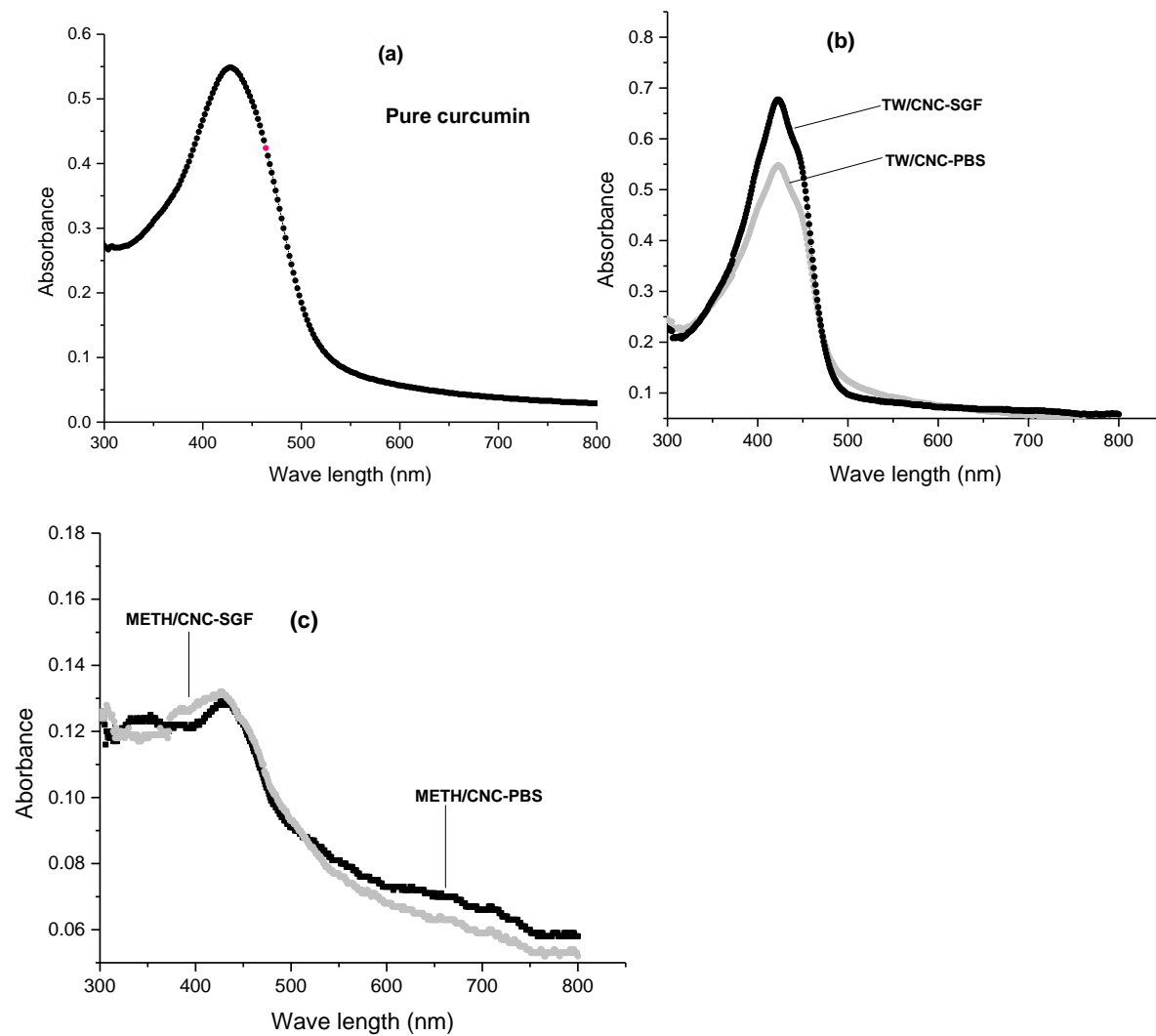


Fig. 9 UV-Vis spectra of: **a** pure curcumin; **b** curcumin release from TW/CNC into PBS and SGF media; **c** curcumin release from METH/CNC into PBS and SGF media

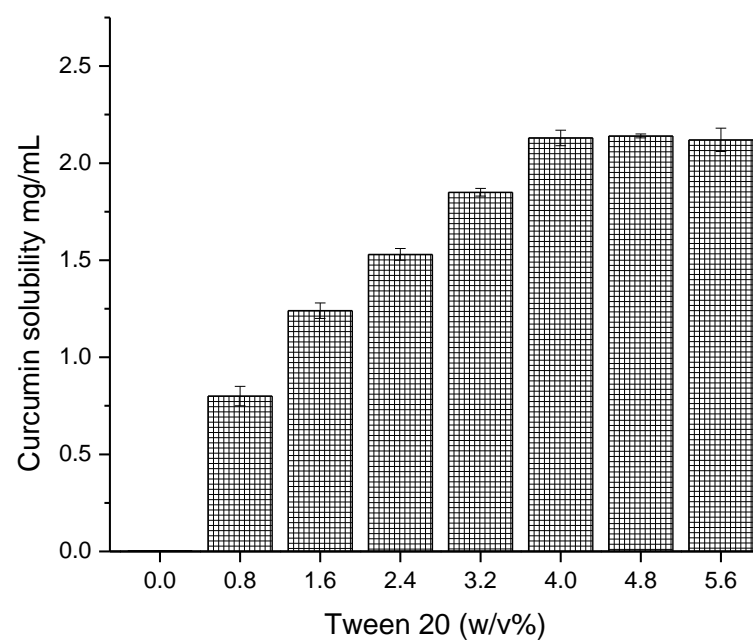


Fig. 10 Solubility of curcumin in distilled water with different concentrations of nonionic surfactant

Table 1 Types of nanocellulose used for the drug release studies (based on the drug loading and releasing medium)

Types of nanocellulose (based on the drug loading and releasing medium)	Weight of nanocellulose (g)	Amount of drug (curcumin) loaded per 1 g of nanocellulose (mg)	Drug loading medium	Drug releasing medium
TW/CNC-SGF	1	7.73	Aqueous solution of Tween 20	Simulated gastric fluid
TW/CNC-PBS	1	7.73	Aqueous solution of Tween 20	Phosphate buffered saline solution
METH/CNC-SGF	1	3.35	Methanolic medium	Simulated gastric fluid
METH/CNC-PBS	1	3.35	Methanolic medium	Phosphate buffered saline solution